

Young tidal dwarf galaxies cannot be used to probe dark matter in galaxies

H. Flores^{1,*}, F. Hammer¹, S. Fouquet², M. Puech¹, P. Kroupa³, Y. Yang¹
and M. Pawlowski⁴

¹ *GEPI, Observatoire de Paris, CNRS-UMR8111, Univ. Paris Diderot, 5 place Jules Janssen, F-92195 Meudon, France*

² *Nicolaus Copernicus Astronomical Center, Bartycka 18, PL-00-716 Warsaw, Poland*

³ *Helmholtz-Institut für Strahlen- und Kernphysik, Rheinische Friedrich-Wilhelms-Universität Bonn, Nussallee 14-16, D-53115 Bonn, Germany*

⁴ *Department of Astronomy, Case Western Reserve University, 10900 Euclid Avenue, Cleveland, OH 44106, USA*

Accepted; Received; in original form

ABSTRACT

The location of dark-matter free, tidal dwarf galaxies (TDGs) in the baryonic Tully Fisher (bTF) diagram has been used to test cosmological scenarios, leading to various and controversial results. Using new high-resolution 3D spectroscopic data, we re-investigate the morpho-kinematics of these galaxies to verify whether or not they can be used for such a purpose. We find that the three observed TDGs are kinematically not virialized and show complex morphologies and kinematics, leading to considerable uncertainties about their intrinsic rotation velocities and their locations on the bTF. Only one TDG can be identified as a (perturbed) rotation disk that it is indeed a sub-component of NGC5291N and that lies at $<1\sigma$ from the local bTF relation. It results that the presently studied TDGs are young, dynamically forming objects, which are not enough virialized to robustly challenge cosmological scenarios.

Key words: dark matter – galaxies: dwarf – galaxies: irregular – galaxies: kinematics and dynamics – galaxies: individual: NGC 5291

1 INTRODUCTION

The Tully-Fisher (TF, Tully & Fisher 1977) relation is probably the most important scaling law of galaxies, relating rotational velocity to luminosity or mass. The baryonic TF (hereafter called bTF) relation is a tight correlation between baryonic mass and rotation velocity (McGaugh et al. 2000; Verheijen 2001) over a considerable range of galaxy velocities, from 20 to 300 km/s (McGaugh et al. 2010). There has been considerable debates about the bTF zero point, slope and evolution and whether these can test cosmological scenarios (see, e.g., McGaugh 2005, 2012; Puech et al. 2010; Dutton et al. 2011; Kroupa 2015 and references therein).

Verifying these scenarios can be also done through comparing the bTF locations of dark-matter free galaxies to that of other galaxies. This is because rotation velocities are naturally linked to the total mass encircled by their measurements, and then, the bTF location of a galaxy provides a direct test of its baryonic fraction (McGaugh et al. 2010). Such a test has been firstly attempted by Bournaud et al. (2007, hereafter B07) by deriving the rotation curves of three tidal dwarf galaxy (TDG, dark-matter free), NGC5291N, S and SW, beyond its optical disk. The flat rotation curve was

used to deduce the total mass and when compared to the baryonic mass, it reveals the presence of a large fraction of unseen material, which B07 dubbed ‘baryonic dark matter’. Gentile et al. (2007) verified the consistency of TDGs with the observed bTF, casting some doubts about the amount of dark matter in the general population of galaxies.

Such a conclusion based on a few objects requires further investigations before being adopted. This has been recently attempted by Lelli et al. (2015) who have reinvestigated the measurements of NGC5291N together with that of five other TDGs, providing a significant offset of all TDGs when compared to the bTF of other galaxies. Though the observations of NGC5291N are those of B07, the new modeling causes a doubling of the gas mass, while the B07 method for establishing the inclined-corrected velocity is claimed to overestimate it by a factor 2. Either the latter casts some doubts about the accuracy of such tests, or it requires to better investigate the observed TDGs and verify the overall methodology to capture their locations in the bTF relation.

In this paper we reinvestigate the nature of TDGs by using 3D-spectroscopy observations with high spectral resolution and signal to noise. In section 2 we describe the 3D observations and the high resolution optical images. Section 3 provides full morpho-kinematics analyses and Section 4 discusses whether or not TDGs can presently be used to

* E-mail: hector.flores@obspm.fr

test cosmological scenarios. Throughout, we adopt $H_0 = 70$ km/s/Mpc, $\Omega_M = 0.3$, and $\Omega_\Lambda = 0.7$.

2 OBSERVATIONS

We observed three TDGs associated to the system NGC 5291 (N, SW and S) with FLAMES/GIRAFFE (ESO run 093.B-0758(A)). We used the ARGUS mode (11"x7" array with 0.52" width microlenses) with the setup LR6 (R=13700 – 21 km/s, a resolution 1.5 better than previous Fabry-Perot observations of Bournaud et al. 2004), and integration times of 3 hours. Observational seeing during 1hr x 3 exposures range from 0.7 to 0.9 arcsec. The data were reduced using the standard ESO pipeline. To test the wavelength calibration, we measured some strong sky lines, showing an error lower than 0.2 km/s. Given the size of TDG NGC 5291 N, we pointed ARGUS in two adjacent regions to construct a larger datacube (final size 41x14 spaxels equivalent to 21".3x7".3, see Fig. 1), and combined the data cubes using standard IRAF tasks. To construct velocity fields and sigma maps (and S/N maps), we used software developed by Flores et al. (2006) and Yang et al. (2008). Each spaxel has been visually checked to avoid sky line and detector residuals (see Flores et al., 2006). Velocity fields and dispersion maps are shown in Fig. 1. We have also retrieved from ESO archive deep images using VLT/FORS2 (ESO run 82.B-0213(A)) and we have reduced the data using the standard ESO pipeline and the IRAF software. They reveal the morphology of TDG NGC5291N, SW and S, with a seeing of 0.7 and 0.8 arcsec, while the photometry was performed using SExtractor and Polyphot within IRAF. Photometric zero points were estimated following the recipe of FORS2.

3 MORPHO-KINEMATIC ANALYSIS OF TDGS

NGC5291 TDGs reveal quite complex and irregular morphologies (see also Fensch et al. 2015) and are lying within an extended diffuse component, which is part of the NGC5291 tidal debris and are also detected in HI (B07). NGC5291N is even more complex revealing at least three components (we call the brightest ones A, B1 and B2), for which photometric measurements are presented in Table 1. This implies that the single object recorded on the DSS image by B07 is in fact made of at least three objects¹. In Figure 1 we retrieve morphology, velocity field, dispersion map and velocity modeling of the three TDGs (NGC5291 N, S and SW), while the second column presents these properties for the sole, dominant component A of NGC5291N.

The position angle (PA) and ellipticity were determined manually and using the ellipse task (under IRAF). We found a difference of ~ 20 degrees between the PA of NGC5291N and its component A. Inclinations calculated from R band have been used to recover the rotation curve (RC). The main reason of this choice is dictated by the physics of rotating

Table 1. Photometry of the three TDGs of NGC 5291 (N, S and SW), the error associated at each magnitude is ± 0.1 . Inclination i and PA were determined from R band image and using kinemetry free. Error of stellar i and PA is ± 5 degrees

	All	N	B1	B2	S	SW
V_{Bessel}	17.37	17.82	19.64	20.21	18.63	18.18
$R_{Special}$	17.61	17.36	19.35	19.50	18.32	17.65
I_{Bessel}	17.56	18.16	19.50	19.93	18.03	17.52
i^1	19	44	–	–	30	32
PA ¹	102	171	–	–	113	-54
i^2	16 ± 10	48 ± 22	–	–	46 ± 38	32 ± 29
PA ²	101 ± 14	163 ± 8	–	–	23 ± 66	-46 ± 58

Notes: ¹ PA and i from stars; ² Assuming PA and i free in the kinemetry.

disks. In a virialized system, here a rotating disk, stars provide the best, indication of the disk center, inclination and PA. Lelli et al. (2015, see their Figures 5 to 7) have provided detailed HI maps of the three systems and have assumed ellipsoidal distribution around the largest velocity gradients, which were assumed to be a rotation. Such a choice leads to rotation centers that are far from the center of the stellar mass distribution (see open crosses in Fig. 1), which has thus no reason to be interpreted as a rotation disk².

The 3D H α flux distribution shows peaks at the three main components (A, B1 and B2) plus smaller knots at different velocities. The median velocity of B1 and B2 are 63 km/s and 41 km/s higher than that of the component A. This confirms that component A can be considered as a single TDG, embedded in a larger gas cloud and will likely merge with the other components in the future, so the final TDG will likely be considerably larger and more massive. NGC5291N is simply a group of TDGs or of cluster complexes (see, e.g., Kroupa 2015). Components B1 and B2 show no strong rotation components (full velocity difference ΔV of 10 and 5 km/s, respectively), which is smaller than the median dispersion (20 and 25 km/s, respectively). Table 2 provides the estimates of velocity and σ for component A as well as for NGC5291S and SW. We have analyzed the corresponding maps using the standard software kinemetry (Krajnović et al. 2006), assuming center, inclination and PA from optical images. The kinematics of NGC5291S and SW are too chaotic (see Fig. 1) to reveal a rotation, even in letting free the dynamical axis. These components are also dominated by quite a large dispersion and by many aspects they are consistent with the complex kinematics class of Flores et al. (2006) and Yang et al. (2008). Fig. 1 evidences that component A is rotating and Fig. 2 presents its rotation

¹ It is indeed a recently formed object (< 350 Myr; see B07) and could be compared to Fig. 10 of Kroupa (2015) for another snapshot of a highly-resolved, young low-mass TDG.

² If a disk galaxy forms from gas lying within a uniform sphere in solid body rotation, the resulting disk has a profile close to an exponential though slightly more concentrated (Mestel 1963; Gunn 1982; Dutton 2009). If it is formed through hierarchical scenario then dissipationless stars are likely aggregating in the center, while viscous, cold gas is more affected by tides (Hopkins et al. 2008). Thus stars virialise within a dynamical time and are expected to better indicate the potential of a galaxy in equilibrium, and up to our knowledge, there is no counter- example of a virialised galaxy having no stars in their center and only having a stellar population in its outskirts.

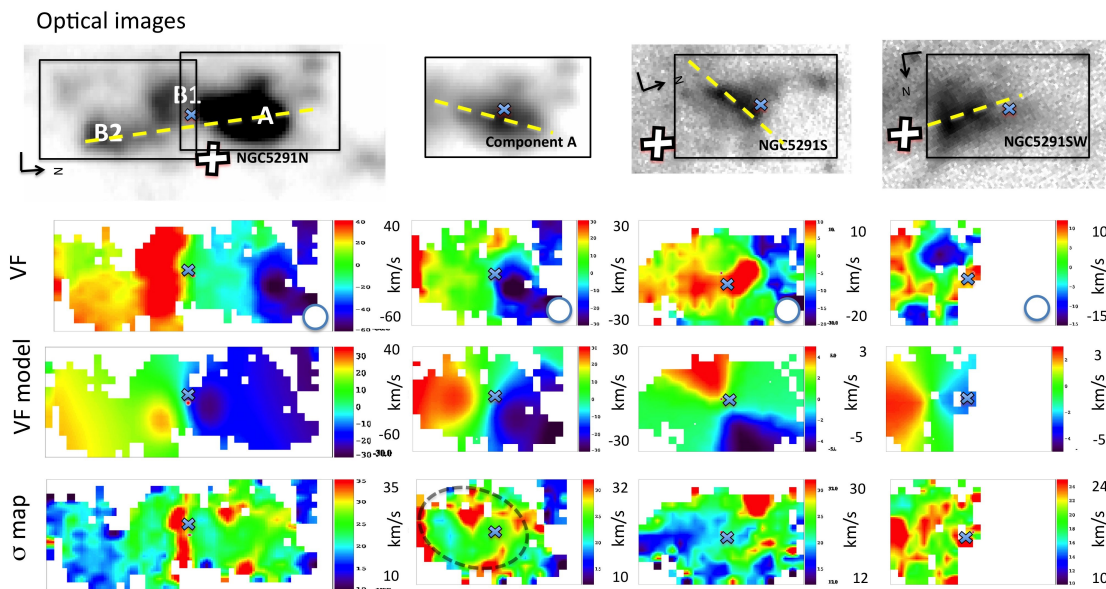


Figure 1. *Top panels:* Finding charts (R band) of each observed TDG candidate: NGC5291N, the component A, NGC5291S and NGC5291SW, respectively. In each finding chart, the position of ARGUS FoV is indicated by as a solid rectangle ($\sim 3.2 \times 2.1$ kpc²). The North-East orientation is given (black arrow) as well as the center (small blue cross). The PA is derived from the optical image (dashed yellow line), and the HI center of rotation assumed by Lelli et al. (2015) is indicated by a large white cross. *Middle-top panels:* Velocity fields from H α that include only spaxels with S/N ≥ 5 and for which we have applied a simple 5×5 linear interpolation for a better visualization, the open circle in the bottom right shows the resolution. *Middle-bottom panels:* Rotation models of the velocity fields assuming the dynamical axis is defined by the stellar disk morphology. *Bottom panels:* Dispersion maps to which we have applied a 5×5 linear interpolation, in the component A a dashed grey line indicates the high [OI]6300/H α distribution from Fensch et al. 2015.

curve together with that of the whole NGC5291N. However component A is not a fully virialized galaxy since it does not show a σ peak at the dynamical center. Such a centered σ peak is expected for a perfect rotation for which the spatial resolution is not sufficient to fully resolved the velocity gradient between the two maximal velocity plateaus (Flores et al. 2006; Yang et al. 2008). Component A kinematics can be classified as a perturbed rotation and this is corroborated by the importance of non circular motions, for which the relative strength to the rotation is determined by the k_5/k_1 ratio³ (see Fig. 2). Values of k_5/k_1 up to ~ 0.1 can be indicative of a rotating component (see, e.g., Krajnović et al. 2006), while values up to ~ 0.5 they are indicative of dominant chaotic motions expected in mergers or close encounters.

There are many clues that the TDGs are indeed forming in a coalescence process, which may not be surprising given the young age of the merger/encounter having occurred in NGC5291 (~ 350 Myr, B07). The surroundings of component A show very high values of [OI]6300/H α (see Fig. 7 of Fensch et al. 2015), which is indicative of shocks. The high [OI]6300/H α distribution coincides with the σ peaks that also form a ring in Fig. 1 (see also Figure 14 of Fensch et

al. 2015). This further suggests that interactions between components are responsible for the shocks, while the shock ring morphology as well as the absence of a large electron density (see Table 2) are not favoring a strong ionized component linked either to supernova outflow or to hot gas in the NGC5291 halo. The fact that the HI gas peak (see the open cross in Fig. 1 and also figure 5 of Lelli et al. 2015) is not aligned with stars and ionized gas in component A is also supporting a pre-merger process as in, e.g., Sengupta et al. (2015, and references therein).

4 THE BARYONIC TULLY FISHER DIAGRAM

Studies of galaxy evolution have strikingly shown a considerable evolution of their kinematics even during a relatively recent past (6 Gyr, Yang et al. 2008; Neichel et al. 2008). Flores et al. (2006) and Puech et al. (2008, 2010) have shown that a significant fraction of these galaxies were strongly offset from the TF and bTF. This is because they are (partly) unvirialized mostly through galaxy interactions and mergers (Hammer et al. 2005, 2009). Merger simulations from Covington et al. (2010) have shown that many of these systems have locations in the TF biased towards low V_{rot} values. Similar offsets for TDGs are reported by Lelli et al. (2015) providing one of the motivations of the present analysis, which reveals that TDG velocity fields are indeed complex (NGC5291S and SW) or show perturbed rotation (component A). Table 2 presents the mass estimates

³ k_5 represents the higher-order deviations from simple rotation and points to complex structures on the maps and it is normalized to the rotation term, k_1 . It is a kinematic analogue of the photometric term that describes the deviation of the isophote shape from an ellipse (disciness and boxiness, Krajnović et al. 2006).

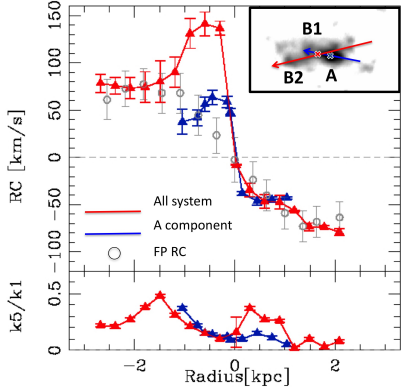


Figure 2. *Top panel:* Rotation curves with error bars of the whole NGC5291N (red line and triangles) and of the A component (blue line and triangles). The RC of B07 (open dots) share similarities with that of the whole NGC5291N, although it seems affected by beam smearing effects (see also Lelli et al. 2015) and it has missed some structures in the velocity field. The insert indicates the adopted PA (red and blue arrows for NGC5291 N and component A, respectively). The last one have the same final V_{rot} , the main difference is found in the structures detected in the central regions of VF. *Bottom panel:* $k5/k1$ ratio along the dynamical axis evidencing that NGC5291N is dominated by non circular motion, while even if the RC of the component A is also asymmetric a V_{rot} can be determined.

Table 2. Physical properties deduced from photometry and ARGUS integrated spectra, electron density estimated from $SII[6716]/SII[6731]$, stellar mass from different prescriptions on star ages, the HI mass estimated using HI observations (Lelli et al., 2015), assuming the HI content is associated to the surface of each stellar component. Masses are given in units of $10^7 M_{\odot}$.

	A	NGC5291 N B1	B2	S	SW
n_e [cm $^{-3}$]	90.0	26.5	<10.0	90.7	1029.3
M_*	$5.1^{+5.1}_{-4.6}$	$1.1^{+1.1}_{-1.0}$	$2.0^{+1.9}_{-1.8}$	$6.6^{+6.6}_{-6.3}$	$19.3^{+19.3}_{-18.8}$
M_{HI}	$20.0^{+4.2}_{-4.6}$	—	—	$7.4^{+2.6}_{-2.5}$	$6.9^{+3.2}_{-3.4}$
M_{mol}	$11^{+11}_{-7.7}$	—	—	$16^{+16}_{-8.2}$	$10^{+10}_{-3.3}$
M_{bar}	36^{+20}_{-17}	—	—	30^{+25}_{-17}	36^{+32}_{-25}
V_{rot}^1	40 ± 10	—	—	6^{+3}_{-3}	8^{+5}_{-4}
V_{rot}^2	28 ± 10	—	—	19^{+14}_{-14}	36^{+34}_{-34}
σ	23 ± 5	—	—	25 ± 5	20 ± 5

Notes: V_{rot} and σ in km/s, 1 Assuming PA and i from stars; 2 Assuming PA and i free in the kinemetry.

of the NGC5291 TDGs. Stellar masses can be calculated from assuming either: (1) that the photometry is dominated by stars coming from the parent galaxies using the Bell et al. (2003) M/L-color relations with I and (V-R) aperture photometry, and, (2) that stellar ages are very young (10 Myr and $\log(M/L)=-1.6$, from Bruzual and Charlot 2003) since TDGs are strongly star forming and Wolf Rayet stars have been detected (Duc & Mirabel 1998). We consider the stellar mass as being the average between the two above values, keeping the difference as the associated uncertainty. HI masses are evaluated using same apertures than for stars.

Large uncertainties are also linked to the molecular gas mass estimates since they are based on a very large PSF (21 arcsec, CO observations from Braine et al. 2001). We have assumed that molecular masses are ranging from high values (attributing all the CO flux related to the TDG) to low values (performing a scaling based on the aperture ratio between the TDG and the Braine et al. 2001 PSF).

Fig. 3 presents the TDG locations in the baryonic Tully Fisher diagram (McGaugh et al. 2000; McGaugh 2005). Error bars on the NGC5291S and SW velocities are very large since there is no evidence that these complex objects are rotating. Indeed we have assumed their velocities range from the ΔV provided by kinemetry (with letting free the PA and i) to the value provided by a modeling based on the observed optical PA (see Fig. 1 and Table 2). The semi virialized nature of component A and its well defined dynamical axis lead to much smaller error bars on its rotation velocity. It follows that (1) the NGC5291 TDGs are not relaxed nor virialized systems and can not be used to robustly test the dark matter content of galaxies by using their locations in the bTF diagram, and (2) their locations are consistent with the local bTF of galaxies, when accounting for uncertainties linked to their kinematics.

5 CONCLUSIONS

A thorough analysis of the three TDG candidates in the recent NGC5291 merger illustrates that there is no reason for them to be interpreted as virialized rotating disk that can be robustly used to test their locations on the bTF relation. This is similar to many distant galaxies that are suspected to be mergers or merger remnants. Lelli et al. (2015) wondered whether the HI disks are in equilibrium based on the comparison of the disk's orbital time versus the interaction times (B07 modeling). However B07 Figure S7 shows mass distributions that are far more regular than observed. Perhaps this is due to the fact that B07 modeled the formation of TDGs using a sticky particles scheme for the gas dynamics, which could be problematic for gas-dominated systems as those studied here. In the following we will refer to Ploekinger et al. (2015) who elaborated a full hydrodynamic treatment high resolution adaptive particle-mesh method by concentrating on individual TDG, including feedback and incorporating for the first time a treatment of discrete stellar populations via the integrated galactic IMF theory, a more robust representation of TDG formation and evolution.

Further attempts to identify their locations in the bTF relation leads to very large error bars for the fully unvirialized systems, while the semi-virialized component A lies close to the bTF of other galaxies (see Fig. 3). We thus conclude that the offsets of the NGC5291 TDGs reported by Lelli et al. (2015) result from a methodological artifact and cannot be straightforwardly used to challenge MOND or another cosmological scenario.

Our conclusion is not changed after examining the three other TDGs studied by Lelli et al. (2015, NGC7252E, NW and VCC2062). The proposed centres are clearly offset from their stellar distribution, which challenges their interpretation as rotating disks. It is likely that all these TDGs are observed too shortly after the merger, revealing TDGs in

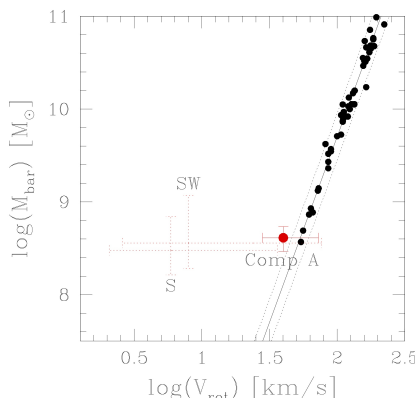


Figure 3. Baryonic TF relation of local galaxies from McGaugh et al. (2000) and McGaugh (2005) together with TDGs and the associated uncertainties. Since NGC5291 S and SW are fully unvirialized we have chosen to represent their points in the right mid-point of their velocity range. Component A appears to be a more mature TDGs and is $< 1\sigma$ from the bTF relation.

their formation process and fed by the gas of the tidal tail instead of virialised systems that may result at least one to three billion years later (see, e.g., Ploekinger et al. 2015 and their Table 2 and Figure 5).

However, the B07 test could still have profound consequences on the cosmological scenarios (see, e.g., Kroupa et al. 2010). This requires to study residuals of much older mergers that could be challenging since tidal tails likely vanish from optical and HI detectability. A possible candidate could be coming from our neighbor, M31, which had probably experienced a major merger, 5.5 Gyr ago (Hammer et al. 2010). In modeling the Magellanic System, Hammer et al. (2015) have shown that its extent towards IC10 could be a residual of such a tidal tail. Then further kinematic studies of IC10 may be very useful to test its baryonic and dark matter content as well as its location on the bTF. Recall that IC10 lies within the M31 plane of satellites (Ibata et al. 2013) and is predicted by the M31 modeling to be a TDG lying within the first tidal tail formed in the ancient merger (see Figure 2 of Hammer et al. 2013). Such studies would also further test the nature of the disk of satellites surrounding the major galaxies, which could be an evidence for a tidal nature of many Local Group dwarfs (Kroupa et al. 2005; Pawlowski et al. 2014).

REFERENCES

Bell, E. F., McIntosh, D. H., Katz, N., & Weinberg, M. D. 2003, *ApJ* S., 149, 289
 Bornauid, F., Duc, P.-A., Amram, P., et al., 2004, *A&A*, 425, 813
 Bornauid, F., Duc, P.-A., Brinks, E., et al. 2007, *Science*, 316, 1166

Bruzual, G. and Charlot, S., 2003, *MNRAS*, 344, 1000
 Braine, J., Duc, P.-A., Lisenfeld, U., et al. 2001, *A&A*, 378, 51
 Covington, M. D., Kassin, S. A., Dutton, A. A., et al. 2010, *ApJ*, 710, 279
 Duc, P. A. & Mirabel, F. 1998, *A&A*, 333, 813
 Dutton, A. A. 2009, *MNRAS*, 396, 121
 Dutton, A. A., van den Bosch, F. C., Faber, S. M., et al. 2011, *MNRAS*, 410, 1660
 Fensch, J., Duc, P.-A., Weilbacher, et al., 2015, *arXiv:1509.08873*
 Flores, H., Hammer, F., Puech et al., 2006, *A&A*, 455, 107
 Gentile, G., Famaey, B., Combes, F. et al., 2007 *A&A*, 472, 25
 Gunn, J. E., 1982, in Bruck H. A., Coyne G. V., Longair M. S., eds, *AC. PSA*, p. 233
 Hammer, F., Flores, H., Elbaz, D., et al. 2005, *A&A*, 430, 115
 Hammer, F., Flores, H., Puech, M., et al. 2009, *A&A*, 507, 1313
 Hammer, F., Yang, Y. B., Wang, J. L., et al. 2010, *ApJ*, 725, 542
 Hammer, F., Yang, Y., Fouquet, S., et al. 2013, *MNRAS*, 431, 3543
 Hammer, F., Yang, Y. B., Flores, et al., 2015, *arXiv:1510.00096*
 Hopkins, P., Cox, T., Hernquist, L. 2008, *ApJ*, 689, 17
 Ibata, R. A., Lewis, G. F., Conn, A. R., et al. 2013, *Nature*, 493, 62
 Krajnović, D., Cappellari, M., de Zeeuw, P. T., & Copin, Y. 2006, *MNRAS*, 366, 787
 Kroupa, P., Theis, C., & Boily, C. M. 2005, *A&A*, 431, 517
 Kroupa, P., Famaey, B., de Boer, K. S., et al. 2010, *A&A*, 523, A32
 Kroupa, P. 2015, *Canadian Journal of Physics*, 93, 169
 Lelli, F., Duc, P.-A., Brinks, E., et al. 2015, *arXiv:1509.05404*
 McGaugh, S. S., Schombert, J. M., Bothun, G. D., & de Blok, W. J. G. 2000, *ApJ Lett.*, 533, L99
 McGaugh, S. S. 2005, *Physical Review Letters*, 95, 171302
 McGaugh, S. S., Schombert, J. M., de Blok, W. J. G., & Zagursky, M. J. 2010, *ApJ Lett.*, 708, L14
 McGaugh, S. S. 2012, *AJ*, 143, 40
 Mestel L., 1963, *MNRAS*, 126, 553
 Neichel, B., Hammer, F., Puech, M., et al. 2008, *A&A*, 484, 159
 Pawlowski, M. S., Famaey, B., Jerjen, H., et al. 2014, *MNRAS*, 442, 2362
 Ploekinger, S., Recchi, S., Hensler, G., & Kroupa, P. 2015, *MNRAS*, 447, 2512
 Puech, M., Flores, H., Hammer, F., et al. 2008, *A&A*, 484, 173
 Puech, M., Hammer, F., Flores, H., et al. 2010, *A&A*, 510, A68
 Sengupta, C., Scott, T. C., Paudel, S., et al. 2015, *arXiv:1509.02614*
 Tully, R. B., & Fisher, J. R. 1977, *A&A*, 54, 661
 Verheijen, M. A. W. 2001, *ApJ*, 563, 694
 Yang, Y., Flores, H., Hammer, F., et al. 2008, *A&A*, 477, 789
 Yang, Y., Hammer, F., Fouquet, S., et al. 2014, *MNRAS*, 442, 2419